Chan, T. M., Gardner, L. and Law, K. H. (2010). Structural design of elliptical hollow sections: a review. Proceedings of the Institution of Civil Engineers - Structures and Buildings. **163(6)**, 391-402.

Structural design of elliptical hollow sections: a review

Gardner, L., Chan, T. M., and Law, K. H.

Abstract

Tubular construction is synonymous with modern architecture. The familiar range of tubular sections, namely square, rectangular and circular hollow sections, has been recently extended to also include elliptical hollow sections. These new sections combine the elegance of circular hollow sections with the improved structural efficiency in bending of rectangular hollow sections, due to the differing flexural rigidities about the two principal axes. Following the introduction of structural steel elliptical hollow sections (EHS), a number of investigations into their structural response have been carried out. This paper presents a state of the art review of recent research on elliptical hollow sections, together with a sample of practical applications. The following aspects are addressed: fundamental research on elastic local buckling and post-buckling, cross-section classification, response in shear, member instabilities, connections and the behaviour of concrete filled EHS. Details of full scale testing and numerical modelling studies are described, and the generation of statistically validated structural design rules, suitable for incorporation into international design codes, is outlined.

Keywords

Design rules, elliptical hollow sections, experimentation, numerical simulations, oval hollow sections, steel structures, tubular construction

List of notation

a	Half of the larger outer diameter of an EHS
A	Gross cross-section area
A_c	Cross-sectional area of the concrete within a concrete-filled steel tube
A_{eff}	Effective cross-section area
A_s	Cross-sectional area of a steel tube
A_v	Shear area
b	Half of the smaller outer diameter of an EHS
D_e	Equivalent diameter
D_{e1}	Equivalent diameter based on Kemper's proposal[9]
D_{e2}	Equivalent diameter proposed by Ruiz-Teran and Gardner[16]
D_{e3}	Equivalent diameter proposed by Zhao and Packer[24]
E	Young's modulus
EHS	Elliptical hollow section
f	Coefficient dependant on the thickness and the larger outer diameter of an EHS
f_{ck}	Compressive concrete strength
f_y	Material yield stress
L_0	Perimeter
$M_{z,Ed}$	Design bending moment about the minor (z-z) axis
$M_{y,Ed}$	Design bending moment about the major (y-y) axis
$M_{el,Rd}$	Elastic moment resistance
$M_{el,z,Rd}$	Elastic moment resistance about the minor axis (z-z) axis
$M_{pl,Rd}$	Plastic moment resistance

$M_{pl,y,Rd}$	Plastic moment resistance about the major (y-y) axis
M_u	Ultimate bending moment
N_{CFT}	Cross-section compression resistance of a concrete-filled EHS
N_{Ed}	Design axial force
$N_{b,Rd}$	Member buckling resistance
N_{cr}	Elastic flexural buckling load
$N_{c,Rd}$	Cross-section compressive resistance
N_u	Ultimate axial load
N_y	Plastic yield load
OHS	Oval hollow section
r	Radius of curvature
R	Rotation capacity
r_{cr}	Critical radius of curvature
r_0	Radius of a circular section with the same perimeter as the corresponding oval
r_{max}	Maximum radius of curvature
r_{min}	Minimum radius of curvature
s	Coordinate along the curved length of an oval
t	Thickness
$V_{pl,Rd}$	Plastic shear resistance
V_u	Ultimate shear force
W_{el}	Elastic section modulus
W_{eff}	Effective section modulus
y	Coordinate along the major (y-y) axis
y-y	Cross-section major axis

z	Coordinate along the minor (z-z) axis
z-z	Cross-section minor axis
ε	Coefficient dependant on the material yield stress
$\bar{\lambda}$	Non-dimensional member slenderness
ν	Poisson's ratio
σ_{cr}	Elastic buckling stress
τ	Yield stress in shear
ξ	Eccentricity of an oval
ψ	Ratio of end stresses

1. INTRODUCTION

Dating back to the mid-nineteenth century, the opening of the Britannia Bridge in the UK (Collins, 1983; Ryall, 1999) in 1850 heralded a new era for structural hollow sections; it was the first major civil engineering application to adopt rectangular hollow sections in the main structural skeleton. Behind the scenes, viable design options involving circular and elliptical hollow sections were also considered during the conceptual design stage. Nine years later, the Engineer Isambard Kingdom Brunel adopted elliptical hollow sections as the primary arched compression elements in one of his masterpieces – the Royal Albert Bridge (Binding, 1997). Subsequently, in 1890, the Forth Railway Bridge (Paxton, 1990) was completed, displaying extensive use of circular hollow sections. The hollow sections employed in these early structures had to be fabricated from plates connected by rivets. As the construction industry continued to evolve, new design and production techniques were developed, and hollow sections are now manufactured as hot-finished structural products with square, rectangular and circular geometries. Now, more than a century after their initial use by Brunel, elliptical hollow sections have emerged as a new addition to the hot-finished product range for tubular construction, and have already been utilised as the primary elements in a number of structural applications. Examples include the Zeeman building at the University of Warwick completed in 2003 (Fig. 1), the Society bridge in Scotland (Corus, 2006) completed in 2005 (Fig. 2) and the main airport terminal buildings in Madrid (Viñuela-Rueda and Martinez-Salcedo, 2006) completed in 2004 (Fig. 3), Cork completed in 2006 (Fig. 4) and London Heathrow completed in 2007 (Figs 5 and 6).

Early analytical research into the structural characteristics of non-circular cylindrical shells initially centred on oval hollow sections (OHS), after which attention turned to sections of

elliptical geometry. The primary focus of these early studies was the elastic buckling and post-buckling response of slender oval and elliptical shells. More recently, following the introduction of hot-finished elliptical tubes of structural proportions, attention has shifted towards the generation of structural performance data through physical testing and numerical simulations and to the subsequent development of structural design rules. The structural scenarios investigated to date include axial compression, bending and shear at both cross-sectional level and member level, concrete-filled tubular construction and connections. This paper presents a state-of-the art review of previous research and current provisions for all aspects of the design of structural steel elliptical hollow sections.

2. GEOMETRY

The recent addition to the family of hot-finished tubular sections is marketed as oval hollow sections. An oval may be described generally as a curve with a smooth, convex, closed 'egg-like' shape, but with no single mathematical definition. Hence, a range of geometric properties, depending on the degree of elongation and asymmetry of ovals exists. The recently introduced sections are, in fact, elliptical in geometry – an ellipse being a special case of an oval – as described later. In early investigations, a number of formulations were examined by Marguerre (1951) to describe the geometry of an oval and the following simplified expression given by equation 1 was adopted by a number of researchers to describe a doubly-symmetric oval cross-section.

$$\frac{1}{r} = \frac{1}{r_0}\left(1 + \xi \cos\left(\frac{4\pi s}{L_0}\right)\right) \tag{1}$$

where r is the radius of curvature at the point s along the curved length of the section, ξ is the eccentricity of the section (ξ= 0 represents a circle, whilst for ξ = 1, the minimum curvature is zero

at the narrow part of the shell cross-section), L_0 is the perimeter of the section and r_0 is the radius of a circular section with the same perimeter.

An ellipse is a special case of an oval and can be described mathematically as

$$\left(\frac{z}{a}\right)^2 + \left(\frac{y}{b}\right)^2 = 1 \tag{2}$$

where y and z are the Cartesian coordinates, a is half of the larger outer diameter and b is half of the smaller outer diameter, as shown in Fig. 7. The aspect ratio of an ellipse is defined as a/b, while the maximum and minimum radii of curvature may be shown to be: $r_{max} = a^2/b$ and $r_{min} = b^2/a$. The ratio between the maximum radius of curvature and the minimum radius of curvature characterises the shape of the ellipse and is given by $(a/b)^3$.

Romano and Kempner (1958) derived a relationship between the eccentricity ξ of an oval and the aspect ratio a/b of an ellipse and concluded that the two shapes, defined by equations (1) and (2), were comparable provided $0 \leq \xi \leq 1$. It is worth noting that for $\xi = 0$, equation (1) exactly represents a circle (i.e. an ellipse with a/b = 1), while for $\xi = 1$, the corresponding aspect ratio is 2.06. In the following discussions, an oval hollow section and an elliptical hollow section are abbreviated to OHS and EHS respectively.

3. ELASTIC LOCAL BUCKLING AND POST-BUCKLING

Extensive analytical work on the elastic buckling and post-buckling of OHS and EHS under axial compression was conducted in the 1950s and 1960s, with the earliest study being performed by Marguerre (1951). Following on from this critical work, Kempner (1962) concluded that the elastic buckling stress of an OHS could be accurately predicted by the buckling stress of a circular

hollow section (CHS) with a radius equal to the maximum radius of curvature of the OHS and that the solution was a lower bound. The post-buckling behaviour of OHS was first studied by Kempner and Chen (1964), who observed that the higher the aspect ratio of the OHS, the more stable the post-buckling behaviour (approaching that of a flat plate) and, the lower the aspect ratio, the more unstable the post-buckling behaviour (approaching that of a circular shell). The stable post-buckling response of sections with high aspect ratios, enabling loads beyond the elastic buckling load to be sustained, was attributed to the ability of the sections to redistribute stresses to their stiffer regions of high curvature upon buckling Kempner and Chen (1966).

The buckling and initial post-buckling behaviour of elliptical hollow sections was first studied by Hutchinson (1968). Hutchinson concluded that Kempner's proposal (Kempner, 1962) whereby the elastic buckling stress of an OHS could be accurately predicted using the classical CHS formulation with an equivalent radius equal to the maximum radius of curvature of the OHS, may also be applied to EHS. Tennyson et al. (1971) carried out physical tests to assess the buckling behaviour of EHS with aspect ratios between 1 and 2. The tests confirmed that elliptical shells with aspect ratios close to unity exhibit unstable post-buckling behaviour and high imperfection sensitivity, resulting in collapse loads below the elastic buckling load. Conversely, while the elliptical sections with an aspect ratio of 2 exhibited initially unstable post-buckling behaviour, the response quickly restabilized, resulting in attainment of collapse loads in excess the initial buckling loads. These findings were corroborated by Feinstein et al. (1971).

The recent introduction of hot-finished EHS has prompted further research, including a re-evaluation of the fundamental elastic buckling and post-buckling characteristics of elliptical shells, principally by means of numerical analysis techniques. While the findings of the previous researchers have been largely confirmed, detailed numerical modelling (Zhu and Wilkinson, 2006;

Ruiz-Teran and Gardner, 2008; Silvestre, 2008) has revealed that use of the maximum radius of curvature in the prediction of the elastic buckling stress of an EHS in compression becomes increasingly inaccurate for higher aspect ratios and thicker tubes, hence, revised expressions have been devised (Ruiz-Teran and Gardner, 2008; Silvestre, 2008). Most recently, the post-buckling stability and imperfection sensitivity of EHS were systematically quantified (Silvestre and Gardner, submitted) in terms of bifurcation angle and slope of ascending post-buckling equilibrium path. This study provides insight for the future development of effective area formulae for local buckling of slender EHS.

4. HOT-FINISHED ELLIPTICAL HOLLOW SECTIONS

Hot finished structural sections of standardized geometries are the staple products employed within the steel construction industry. Such sections are now available in elliptical profiles with outer dimensions ranging from 150×75 mm to 500×250 mm. thicknesses range between 4 mm and 16 mm and all sections have an aspect ratio of two. Approximate formulae for the determination of geometric properties for elliptical hollow sections (EHS) are provided in the European product standard, EN 10210-2 (2006). The following sections summarise the latest research findings and design proposals for elliptical hollow sections in a range of structural scenarios. Extensive laboratory testing and numerical modelling has been conducted on EHS over the past few years. A summary of the physical tests that have been performed is reported in Table 1. These include stub columns tests, in-plane bending tests, combined bending and shear tests, combined axial load and bending tests, column flexural buckling tests, connection tests and tests on concrete-filled tubes. These tests have been supplemented by numerically generated structural performance data and employed in the development and verification of design rules. A series of tests have also been

carried out on cold-formed stainless steel EHS and corresponding design guidance has been developed (Theofanous et al., 2009a, 2009b; Lam et al., in press).

5. CROSS-SECTION BEHAVIOUR

5.1 Compression

Axial compression represents one of the fundamental loading arrangements for structural members. For cross-section classification under pure compression, of primary concern is the occurrence of local buckling before yielding. Cross-sections that reach the yield load are considered Class 1-3 (fully effective), while those where local buckling prevents attainment of the yield load are Class 4 (slender). For uniform compression, a cross-section slenderness parameter has been determined by consideration of the elastic critical buckling stress.

The elastic critical buckling stress σ_{cr} of a uniformly compressed OHS/EHS may be reasonably approximated by substituting the expression for the maximum radius of curvature r_{max} into the classical buckling stress of a circular cylinder (Kempner, 1962; Hutchinson, 1968), as given by equation (3).

$$\sigma_{cr} = \frac{E}{\sqrt{3(1-\nu^2)}(r_{max}/t)} \tag{3}$$

where E is the Young's modulus, ν is the Poisson's ratio and t is the thickness of the shell. This assumes that buckling initiates at the point of maximum radius of curvature and ignores the restraining effect of the surrounding material of lower radius of curvature and the influence of the boundary conditions. For an elliptical section, r_{max} may be shown to be equal to a^2/b. It has therefore been proposed (Chan and Gardner, 2008a) that under pure compression, the cross-section slenderness of an elliptical hollow section is defined as

$$\frac{D_{e1}}{t\varepsilon^2} = 2\frac{(a^2/b)}{t\varepsilon^2} \tag{4}$$

where D_{e1} is the equivalent diameter based on Kempner's proposal[9] for σ_{cr} and $\varepsilon^2 = 235/f_y$ to allow for a range of yield strengths.

Further research on the elastic buckling of elliptical tubes (Ruiz-Teran and Gardner, 2008) revealed inaccuracies in Kempner's predictive formula (equation (3)) for EHS with higher aspect ratios and tube thickness. Following analytical and numerical studies, an improved expression for the elastic buckling stress of a uniformly compressed EHS was derived and hence a revised expression for the equivalent diameter, given by equation (5), was proposed.

$$D_{e2} = 2a\left[1 + f\left(\frac{a}{b} - 1\right)\right] \quad \text{where} \quad f = 1 - 2.3\left(\frac{t}{2a}\right)^{0.6} \tag{5}$$

The corresponding cross-section slenderness of a compressed elliptical hollow section may therefore be defined as

$$\frac{D_{e2}}{t\varepsilon^2} = 2a\frac{\left[1 + f\left(\frac{a}{b} - 1\right)\right]}{t\varepsilon^2} \tag{6}$$

where D_{e2} is the equivalent diameter proposed by Ruiz-Teran and Gardner (2008).

The above slenderness measures apply over the full range of practical aspect ratio of EHS (say $1 \leq a/b \leq 4$) and are comparable with the current treatment of circular hollow sections, in the sense that for the case of a/b = 1, both give an equivalent diameter equal to the actual diameter of a CHS. A comparison of CHS and EHS test data (Chan and Gardner, 2008a; Zhao and Packer, 2009;

Giakoumelis and Lam, 2004; Teng and Hu, 2007; Sakino et al., 2004; Tutuncu and O'Rourke, 2006) in compression is shown in Fig. 8, while a typical experimental failure mode for a compressed EHS is shown in Fig 9. For EHS, the results are plotted on the basis of the two equivalent diameters D_{e1} (Chan and Gardner, 2008a) and D_{e2} (Ruiz-Teran and Gardner, 2008). Regression curves have also been added for the three data sets in the figure. The results demonstrate that both slenderness parameters for EHS are conservative in comparison to CHS, but the proposal by Ruiz-Teran and Gardner (2008) yields closer agreement between the two section types, and increases the number of sections from the current range of EHS being fully effective, and is thus more accurate and appropriate for design. On this basis, it was recommended that, EHS may be classified in compression using the current CHS slenderness limit of 90 in EN 1993-1-1 (2005) and the equivalent diameter and slenderness parameter defined by equations (5) and (6). The more straightforward measure of slenderness based on D_{e1} (equation (4)) has been adopted in the SCI/BSCA design tables (SCI/BSCA, 2008), commonly referred to as the 'blue book'.

An alternative approach to the cross-section classification of EHS was proposed by Zhao and Packer (2009), whereby the structural response was likened to that of RHS comprising flat plates rather than a circular tube, and the degree of curvature in the section ignored. Hence, the proposed slenderness measure, based on an equivalent diameter $D_{e3} = (2a - 2t)$ was given by equation (7),

$$\frac{D_{e3}}{t\varepsilon} = \frac{2(a - t)}{t\varepsilon} \tag{7}$$

and it was recommended that the Class 3 slenderness limit for flat internal elements in compression of 42 (EN 1993-1-1, 2005) should apply. It is worth nothing that, for an aspect ratio $a/b = 2$, assuming the thickness of the section to be small, D_{e3} is approximately half that of D_{e1} and D_{e2} and the slenderness limit for flat elements in compression is approximately half of that for a

CHS. Hence, both approaches will typically yield similar results. However, for lower aspect ratio, use of D_{e3} with the RHS slenderness limit will be increasingly conservative. A further interesting difference between the two approaches lies in the use of the ε factor, which is employed to modify the section slenderness based on material strength f_y. Assuming shell-like behaviour D_{e1} and D_{e2} are normalised by ε^2, while based on plate-like behaviour D_{e3} is normalised by ε. The reality is likely to be intermediate between these two extremes, and will clearly be dependent on the aspect ratio of the section.

Failure to reach the yield load in compression due to the occurrence of local buckling is generally treated in design using either an effective stress or an effective area approach, with recent trends favouring the latter. A preliminary effective area formula (equation (8)) for Class 4 (slender) elliptical hollow sections was proposed by Chan and Gardner (2008a) and found to be suitable for design for the current practical range of EHS.

$$A_{eff} = A\left[\frac{90}{D_e/t}\frac{235}{f_y}\right]^{0.5} \tag{8}$$

This proposal, taking $D_e = 2a^2/b$, has been adopted in the SCI/BCSA design tables (SCI/BSCA, 2008).

5.2 Bending

For minor (z-z) axis bending, similar to axial compression, local buckling initiates at the point of greatest radius of curvature which coincides with the most heavily compressed part of the cross-section. It was therefore proposed that the same cross-section slenderness parameter given by equation (4) can also be adopted for EHS in minor axis bending; this proposal was supported by available test data and adopted in the SCI/BSCA design tables (SCI/BSCA, 2008). For bending about the major (y-y) axis, local buckling initiates, in general, neither at the point of maximum

radius of curvature (located now at the neutral axis of the cross-section with negligible bending stress) nor at the extreme compressive fibre, since this is where the section is of greatest stiffness (i.e. minimum radius of curvature). A critical radius of curvature r_{cr} was therefore sought to locate the point of initiation of local buckling (Gerard and Becker, 1957). This was achieved by optimizing (i.e. finding the maximum value of) the function composed of the varying curvature expression and an elastic bending stress distribution. The theoretical point of initial of buckling, assuming a linear elastic stress distribution was found at $r_{cr} = 0.65a^2/b$. This result was modified (Chan and Gardner, 2008b) to provide better prediction of observed physical behaviour, to yield r_{cr} equal to $0.4a^2/b$ (see Fig. 10). As the aspect ratio of the section reduces (i.e. the section becomes more circular), the point of initiation of buckling tends towards the extreme compressive fibre of the section. This is reflected by a transition in r, to the local radius of curvature at the extreme fibre where $r = b^2/a$, at an aspect ratio $a/b = 1.357$. Thus, the slenderness parameters for major axis bending proposed by Chan and Gardner (2008b), and adopted in the SCI/BCSA design tables (SCI/BSCA, 2008), are given by equations (9) and (10).

$$\frac{D_e}{t\varepsilon^2} = 0.8\frac{(a^2/b)}{t\varepsilon^2} \qquad \text{for } a/b > 1.357 \qquad (9)$$

$$\frac{D_e}{t\varepsilon^2} = 2\frac{(b^2/a)}{t\varepsilon^2} \qquad \text{for } a/b \leq 1.357 \qquad (10)$$

Based on their proposed measures of slenderness (equations (4), (9) and (10)), Chan and Gardner (2008b) assessed the applicability of current CHS slenderness limits to EHS, with the following criteria to demark the classes of cross-section: Class 1 sections were required to reach the plastic moment capacity $M_{pl,Rd}$ and passes a minimum rotation capacity R of 3, Class 2 sections were required only to reach $M_{pl,Rd}$, while Class 3 sections were required to reach the elastic moment capacity $M_{el,Rd}$ else the sections were Class 4. By means of comparison with available test and FE

data, the current CHS slenderness limits given in EN 1993-1-1 (2005) of $D_e/t\varepsilon^2 = 50$ for Class 1, 70 for Class 2 and 90 for Class 3 were found to be suitable for EHS. It was further recommended that the Class 3 limit of 90 could be reduced to 140 for both CHS and EHS.

An interim effective section modulus formula, given by equation (11), W_{eff} for Class 4 (slender) elliptical hollow sections was also proposed and found to be safely applicable when compared to test and FE results.

$$W_{eff} = W_{el}\left[\frac{140}{D_e/t}\frac{235}{f_y}\right]^{0.25} \tag{11}$$

5.3 Combined compression and bending

For cross-section classification under combined compression and bending (Gardner and Chan, 2007), designers may initially simply check the cross-section against the most severe loading case of pure compression. If the classification is Class 1, then there is no benefit to be gained from checking against the actual stress distribution. Similarly, if plastic design is not being utilized, there would be no benefit in re-classifying a Class 2 cross-section under the actual stress distribution. Under combined compression and minor axis bending, clearly local buckling will initiate in the region of the maximum radius of curvature, similar to the case of pure compression and pure minor axis bending. Under combined compression and major axis bending, the critical radius of curvature (i.e. the point of initiation of local buckling) will shift towards the centroidal axis as the compressive part of the loading increases. This effect is shown in Fig. 11, where z/a is the normalised distance of r_{cr} from the centroid of the section and $\psi = \sigma_2/\sigma_1$ is the ratio of the end stresses between which a linear gradient is considered. Note that Fig. 11 shows the theoretical elastic buckling response, which has not be adjusted in the light of experimental observations, as described for the case of pure major axis bending in the previous section. For $\psi = 1$, which

corresponds to pure compression, buckling initiates at z/a = 0 (i.e. the centroid of the section) for all aspect ratios. As ψ decreases, the position of initiation of buckling migrates up the section where the greater stresses exist. This migration is more rapid in sections of low aspect ratio where there is less variation in radius curvature around the section.

For Class 3 sections under combined loading, EN 1993-1-1 (2005) provides the linear interaction formula, given by equation (12). When compared to tests results, this interaction formula was shown (Chan and Gardner, 2009b) to be applicable to EHS.

$$(N_{Ed}/N_{c,Rd}) + (M_{z,Ed}/M_{el,z,Rd}) \leq 1.0 \quad (12)$$

where $M_{z,Ed}$ is the design bending moment about the minor (z-z) axis and $M_{el,z,Rd}$ is the design elastic bending resistance about the minor (z-z) axis, N_{Ed} is the design axial force and $N_{c,Rd}$ is the design cross-section resistance under uniform compression.

In the plastic regime, Nowzartash and Mohareb (2009) derived interaction surfaces for EHS under combined compression and bending about the two principal axes. Their proposed interaction expression is given by equation (13).

$$(M_{y,Ed}/M_{pl,y,Rd})^2 + 2(N_{Ed}/N_{c,Rd})^{1.75} + (N_{Ed}/N_{c,Rd})^{3.5} \leq 1.0 \quad (13)$$

where $M_{y,Ed}$ is the design bending moment about the major (y-y) axis and $M_{pl,y,Rd}$ is the design plastic bending resistance about the major (y-y) axis.

The two interaction formulations (equation (12) for Class 3 sections and equation (13) for Class 1 and 2 sections) have been plotted, together with available test data, in Fig. 12, and may be seen to provide safe-side predictions of the resistance of EHS to combined bending and axial compression.

5.4 Shear and combined bending and shear

The plastic shear resistance of an EHS was derived by Gardner et al. (2008) based on the assumption that shear stresses at yield are distributed uniformly around the section and acting tangentially to the surface (see Fig. 13). For transverse loading in the y-y direction, this yielded a plastic shear resistance $V_{pl,Rd}$ equal to twice the product of the vertical projection of the elliptical section (measured to the centreline of the thickness) and the thickness given by 2(2b-t)t multiplied by the yield stress in shear τ_y. Likewise, for transverse load in the z-z direction (see Fig. 13), the corresponding projected area is equal to 2(2a-t)t. Therefore, for an elliptical hollow section of constant thickness, the shear area A_v may be defined by equations 14 and 15. These proposed shear areas have been adopted in the SCI/BCSA design tables (SCI/BSCA, 2008).

$$A_v = (4b-2t)t \qquad \text{for loading in the y-y direction} \qquad (14)$$

$$A_v = (4a-2t)t \qquad \text{for loading in the z-z direction} \qquad (15)$$

Test results on EHS under combined bending and shear are plotted in Fig. 14. The results demonstrate that where the shear force is less than half the plastic shear resistance $V_{pl,Rd}$, the effect of shear on the bending moment resistance is small. Conversely, for high shear force (greater than 50% of $V_{pl,Rd}$), there is a degradation of the bending moment resistance. The proposed moment-shear interaction (Gardner et al., 2008) derived from EN 1993-1-1 (2005) has been plotted in Fig. 14 and shows good agreement with the experimental data.

6. MEMBER BEHAVIOUR

6.1 Flexural column buckling

Flexural buckling of EHS columns has been studied by Chan and Gardner (2009a). A total of 24 experiments were performed – 12 buckling about the major axis and 12 about the minor axis. The experimental data were supplemented with additional structural performance data generated from validated numerical models. The combined results are shown in Fig. 15, where on the vertical axis, the buckling load has been normalised by the cross-section resistance, and on the horizontal axis is the member slenderness $\bar{\lambda} = (Af_y / N_{cr})^{0.5}$, N_{cr} being the elastic buckling load of the column. The results were found to follow a similar trend to buckling data for hot-finished CHS columns, which have been added to the graph. Supported by statistical analysis, it was therefore proposed that the buckling curve (curve 'a' in EN 1993-1-1, 2005) for hot-finished CHS could also be safely applied to hot-finished EHS. This proposal has been adopted in the SCI/BCSA design tables (SCI/BSCA, 2008).

6.2 Lateral torsional buckling

Lateral torsional buckling is the member buckling mode associated with laterally unrestrained beams loaded about their major axis. The closed nature of tubular sections results in high torsional stiffness, making them inherently resistant to buckling modes featuring torsional deformations. For circular sections, lateral torsional buckling is not possible, while for EHS with low aspect ratios, it is of no practical concern. However, for higher aspect ratios, the disparity in major and minor axis flexural stiffness grows, and susceptibility to lateral torsional buckling increases. Initial studies have indicated that lateral torsional buckling should be considered in EHS with aspect ratios a/b higher than about 3.

7. CONNECTIONS

A number of recent studies have been performed to examine the behaviour of connections to and between elliptical hollow section members. Two general connection types have been considered; the first featuring fully welded connections between elliptical tubes in truss-type applications, and the second relating to gusset plate connections which might be employed in trusses or for diagonal bracing members in steel framed buildings. The following two sub-sections describe the latest research findings in these areas.

7.1 Welded truss-type connections

The first full-scale experimental studies on connections between structural steel elliptical hollow sections were performed by Bortolotti et al. (2003) and Pietrapertosa and Jaspart (2003). The test configurations mimicked fully welded brace-to-chord connections typically found in trusses. The experimental data were utilised to validate numerical models, which were subsequently employed to perform parametric analyses. Existing design rules for equivalent RHS and CHS connections were reviewed and preliminary observations and recommendations on their suitability for EHS connections were made. Additional numerical analyses, covering a wider range of variables, were carried out by Choo et al. (2003), who concluded that the ring model originally devised for CHS joints (Togo, 1967) may also applied to describe the behaviour of EHS joints, and that with appropriate orientation of brace and chord member, axially loaded EHS connections can achieve higher capacities than equivalent CHS connections. Further research on welded truss-type connections featuring EHS is underway.

7.2 Gusset plates connections

The behaviour of gusset plate connections to EHS members has been investigated experimentally and numerically. Two general configurations have been studied; the first considers gusset plates welded to the sides of EHS members, representing, for example, connections to chord members in trusses, while the second examines gusset plates employed in end connections, for example to bracing members in frames or web members in trusses.

For the first configuration, six full-scale tests were conducted by Willibald et al. (2006a), exploring different orientations and different connection details, covering both branch and through plate connections, orientated longitudinally and transversely, and connected to both the wider and narrower sides of the EHS. Comparisons of the test results with existing RHS and CHS design formulae revealed that neither fully represented the behaviour of EHS connections, but that the RHS provisions could be conservatively adopted.

For the second configuration, five full-scale tests on gusset plate connections to the ends of EHS members were reported by Willibald et al. (2006b), together with eight similar tests on end connections to CHS members. Both slotted tube and slotted plate connection details were examined, with plates orientated to span either the smaller or larger EHS diameter (see Fig. 16). Failure of all specimens was by either circumferential fracture of the tube or tear out of the base material of the tube along the weld. The five test results were utilised by Martinez-Saucedo et al. (2008) for the validation of numerical models, which were subsequently used to perform parametric studies to enable a wider range of variables, including weld length, connection eccentricity and EHS diameter, to be examined. Based on the findings, design recommendations for slotted end EHS connections, accounting for a number of possible failure modes, were proposed.

8. CONCRETE-FILLED EHS

An increasingly popular means of improving structural efficiency in tubular construction is through concrete infilling (Shanmugam and Lakshmi, 2001). Concrete infilling of steel tubes provides enhanced strength and stiffness, greater resistance to local buckling and improved performance in fire.

The behaviour of filled elliptical tubes has been investigated analytically (Bradford and Roufegarinejad, 2007), experimentally (Yang et al., 2008; Zhao and Packer, 2009) and numerically (Jamaluddin et al., 2009). The studies examined composite load-carrying capacity, ductility, level of concrete confinement afforded by the elliptical tube and the simulated effect of concrete shrinkage. A model for predicting the strength of the confined concrete was also proposed by Dai and Lam (2010). The response of concrete-filled EHS was found, in general, to be intermediate between that of concrete-filled SHS/RHS and CHS (Yang et al., 2008; Zhao and Packer, 2009). An analytical model to predict the strength of confined concrete in elliptical tubes, based on a modification to a previously devised model for concrete columns with elliptical reinforcement hoops (Campione and Fossetti, 2007), was proposed and verified (Yang et al., 2008). As anticipated, thicker tubes were found to provide greater confinement and improved ductility. Existing design rules for concrete-filled SHS/RHS, including those provided in EN 1994-1-1 (2004), were shown to be safely applicable to concrete-filled EHS, while the corresponding rules for CHS generally resulted in an over prediction of capacity. It was concluded (Yang et al., 2008; Zhao and Packer, 2009) that the cross-section compression resistance of a concrete-filled EHS N_{CFT} could be most accurately predicted by a simple summation of the steel and concrete resistances (equation (16)), as recommended for SHS and RHS in EN 1994-1-1 (2004).

$$N_{CFT} = A_s f_y + A_c f_{ck} \quad (16)$$

where A_s is the cross-sectional area of the steel tube, f_y is the yield strength of the steel, A_c is the cross-sectional area of the concrete and f_{ck} is the compressive concrete strength.

9. CONCLUSIONS

A series of research programmes have been recently conducted around the world following the introduction of elliptical hollow sections as hot-finished structural steel construction products. These studies have included fundamental analytical investigations of the buckling and post-buckling response of elliptical tubes building on earlier studies performed in the 1960s, full-scale experimental programmes on members and connections and detailed numerical simulations. A total of over 150 tests have been performed, supplemented by a multiplicity of numerically generated structural performance data. On the basis of the findings of these studies, a number of proposals for structural design rules have been made. Many of these design rules have been incorporated into industry design guidance (SCI/BSCA, 2008). In this paper, a state of the art review of this research has been presented; it is concluded that the design recommendations made are suitable for incorporation into international structural design standards.

REFERENCES

Binding J (1997) *Brunel's Royal Albert Bridge*. Twelveheads Press.

Bortolotti E, Jaspart JP, Pietrapertosa C, Nicaud G, Petitjean PD and Grimault JP (2003) Testing and modelling of welded joints between elliptical hollow sections. *Proceedings of the 10th International Symposium on Tubular Structures*, Madrid, 259–266.

Bradford MA and Roufegarinejad A (2007) Elastic local buckling of thin-walled elliptical tubes containing elastic infill material. *Interaction and Multiscale Mechanics* **1(1):** 143–156.

Campione G and Fossetti M (2007) Compressive behaviour of concrete elliptical columns confined by single hoops. *Engineering Structures* **29(3):** 408–417.

Chan TM and Gardner L (2008a) Compressive resistance of hot-rolled elliptical hollow sections. *Engineering Structures* **30(2):** 522–532.

Chan TM and Gardner L (2008b) Bending strength of hot-rolled elliptical hollow sections. *Journal of Constructional Steel Research* **64(9):** 971–986.

Chan TM and Gardner L (2009a) Flexural buckling of elliptical hollow section columns. *Journal of Structural Engineering ASCE* **135(5):** 546–557.

Chan TM and Gardner L (2009b) Structural behaviour of elliptical hollow sections under combined actions. *Proceedings of the 6th International Conference on Advances in Steel Structures*, Hong Kong, China, 253–260.

Choo YS, Liang JX, and Lim LV (2003) Static strength of elliptical hollow section X-joint under brace compression. *Proceedings of the 10th International Symposium on Tubular Structures*, Madrid, 253–258.

Collins AR, Editor (1983) *Structural Engineering – Two centuries of British achievement*. The Institution of Structural Engineers, Tarot Print.

Corus (2006) *Celsius® 355 Ovals*. Corus Tubes – Structural & Conveyance Business.

Dai X and Lam D (2010) Numerical modelling of the axial compressive behaviour of short concrete-filled elliptical steel columns. *Journal of Constructional Steel Research*. **66(7):** 931-942.

EN 1993-1-1 (2005) *Eurocode 3: Design of steel structures – Part 1-1: General rules and rules for buildings*. CEN.

EN 1994-1-1 (2004) *Eurocode 4: Design of composite steel and concrete structures – Part-1-1: General rules and rules for buildings*. CEN.

EN 10210-2 (2006) *Hot finished structural hollow sections of non-alloy and fine grain steels – Part 2: Tolerances, dimensions and sectional properties*. CEN.

Feinstein G, Erickson B and Kempner J (1971) Stability of oval cylindrical shells. *Experimental Mechanics* **11(11):** 514–520.

Gardner L and Chan TM (2007) Cross-section classification of elliptical hollow sections. *Steel and Composite Structures* **7(3):** 185–200.

Gardner L, Chan TM and Wadee MA (2008) Shear response of elliptical hollow sections. *Proceedings of the Institution of Civil Engineers - Structures and Buildings* **161(6):** 301–309.

Gerard G and Becker H (1957) Handbook of structural stability: Part III – Buckling of curved plates and shells. *NACA Technical Note* 3783.

Giakoumelis G and Lam D (2004) Axial capacity of circular concrete-filled tube columns. *Journal of Constructional Steel research* **60(7):** 1049–1068.

Hutchinson JW (1968) Buckling and initial postbuckling behaviour of oval cylindrical shells under axial compression. *Journal of Applied Mechanics* **35(1):** 66–72.

Jamaluddin N, Lam D and Ye J (2009) Finite element analysis of elliptical stub CFT columns. *Proceedings of the 9th International Conference on Steel Concrete and Hybrid Structures – ASCCS*, Leeds, UK, 265–270.

Kempner J (1962) Some results on buckling and postbuckling of cylindrical shells. *Collected Papers on Instability of Shell Structures*. NASA TND–1510, 173–186.

Kempner J and Chen YN (1964) Large deflections of an axially compressed oval cylindrical shell. *Proceedings of the 11th International Congress of Applied Mechanics*, Munich, 299–305.

Kempner J and Chen YN (1966) *Buckling and postbuckling of an axially compressed oval cylindrical shell*. Department of Aerospace Engineering and Applied Mechanics, Polytechnic Institute of Brooklyn, PIBAL Report 917.

Lam, D., Gardner, L. and Burdett, M. (2010). Behaviour of axially loaded concrete-filled stainless steel elliptical stub columns. *Advances in Structural Engineering*. **13(3):** 493-500.

Marguerre K (1951) Stability of the cylindrical shell of variable curvature. *NACA Technical Memorandum* 1302.

Martinez-Saucedo G, Packer JA and Zhao XL (2008) Static design of elliptical hollow section end-connections. *Proceedings of the Institution of Civil Engineers - Structures and Buildings* **161(2):** 103–113.

Nowzartash F and Mohareb M (2009) Plastic interaction relations for elliptical hollow sections. *Thin-Walled Structures* **47(6-7):** 681–691.

Paxton R, Editor (1990) *100 years of the Forth Bridge*. Thomas Telford.

Pietrapertosa C and Jaspart JP (2003) Study of the behaviour of welded joints composed of elliptical hollow sections. *Proceedings of the 10th International Symposium on Tubular Structures*, Madrid, 601–608.

Romano FJ and Kempner J (1958) *Stress and displacement analysis of a simply supported, noncircular cylindrical shell under lateral pressure*. Department of Aeronautical Engineering and Applied Mechanics, Polytechnic Institute of Brooklyn, PIBAL Report 415.

Ruiz-Teran AM and Gardner L (2008) Elastic buckling of elliptical tubes. *Thin-Walled Structures* **46(11):** 1304–1318.

Ryall MJ (1999) Britannia Bridge: From concept to construction. *Civil Engineering, Institution of Civil Engineers* **132(2-3):** 132–143.

Sakino K, Nakahara H, Morino S and Nishiyama I (2004) Behavior of Centrally Loaded concrete-filled steel tube short columns. *Journal of Structural Engineering ASCE* **130(2):** 180–188.

SCI/BSCA (2008) *Steel Building Design: Design Data in accordance with Eurocodes and the UK National Annexes*. The Steel Construction Institute and British Constructional Steelwork Association, SCI Publication P363.

Shanmugam NE and Lakshmi B (2001) State of the art report on steel-concrete composite columns. *Journal of Constructional Steel Research* **57(10):** 1041–1080.

Silvestre N (2008) Buckling behaviour of elliptical cylindrical shells and tubes under compression. *International Journal of Solids and Structures* **45(16):** 4427–4447.

Silvestre N and Gardner L (submitted) Elastic local post-buckling of elliptical tubes. *Journal of Constructional Steel Research.*

Teng JG and Hu YM (2007) Behaviour of FRP-jacketed circular steel tubes and cylindrical shells under axial compression. *Construction and Building Materials* **21(4):** 827–838.

Tennyson RC, Booton M and Caswell RD (1971) Buckling of imperfect elliptical cylindrical shells under axial compression. *AIAA Journal* **9(2):** 250–255.

Theofanous M, Chan TM and Gardner L (2009a) Structural response of stainless steel oval hollow section compression members. *Engineering Structures* **31(4):** 922–934.

Theofanous M, Chan TM and Gardner L (2009b) Flexural behaviour of stainless steel oval hollow sections. *Thin-Walled Structures* **47(6-7):** 776–787.

Togo T (1967) *Experimental study on mechanical behaviour of tubular joints*. PhD thesis, Osaka University, Japan.

Tutuncu I and O'Rourke TD (2006) Compression Behavior of Nonslender Cylindrical Steel Members with Small and large-Scale Geometric Imperfections. *Journal of Structural Engineering ASCE* **132(8):** 1234–1241.

Viñuela-Rueda L and Martinez-Salcedo J (2006) Steel structure and prestressed façade of the new terminal building. *Hormigón Y Acero* **239(1):** 71–84.

Willibald S, Packer JA, Voth AP and Zhao X (2006a) Through-plate joints to elliptical and circular hollow sections. *Proceedings of the 11th International Symposium on Tubular Structures,* Quebéc City, Canada, 221–228.

Willibald S, Packer JA and Martinez-Saucedo G (2006b) Behaviour of gusset plate connections to ends of round and elliptical hollow structural section members. *Canadian Journal of Civil Engineering* **33(4):** 373–383.

Yang H, Lam D and Gardner L (2008) Testing and analysis of concrete-filled elliptical hollow sections. *Engineering Structures* **30(12):** 3771–3781.

Zhao XL and Packer JA (2009) Tests and design of concrete-filled elliptical hollow section stub columns. *Thin-Walled Structures* **47(6-7):** 617–628.

Zhu Y and Wilkinson T (2006) Finite element analysis of structural steel elliptical hollow sections in pure compression. *Proceedings of the 11th International Symposium on Tubular Structures*, Québec City, 179–186.

Figure captions

Fig. 1: Zeeman Building, University of Warwick (2003)

Fig. 2. Society Bridge, Scotland (2005)

Fig. 3. Barajas Airport, Madrid (2004)

Fig. 4. Cork Airport, Ireland (2006)

Fig. 5. Heathrow Airport, London (2007)

Fig. 6. Heathrow Airport (detail), London (2007)

Fig. 7. Geometry of an ellipse

Fig. 8. Comparison of different equivalent diameters employed in EHS slenderness parameters

Fig 9. Typical cross-section failure mode in compression

Fig. 10. Modified location of critical radius of curvature for EHS with a/b = 2 in major axis bending

Fig. 11. Theoretical variation in position of r_{cr} with aspect ratio a/b and stress distribution ψ

Fig. 12. Test results and interaction curves for combined bending and axial compression

Fig. 13. Derivation of plastic shear area for EHS

Fig. 14. Test results and interaction diagram for EHS under combined bending and shear

Fig. 15. EHS column buckling test results and proposed design curve

Fig. 16. Slotted end EHS connections

Table captions

Table 1. Summary of experiments performed on elliptical hollow sections

Fig. 1: Zeeman Building, University of Warwick (2003)

Fig. 2. Society Bridge, Scotland (2005)

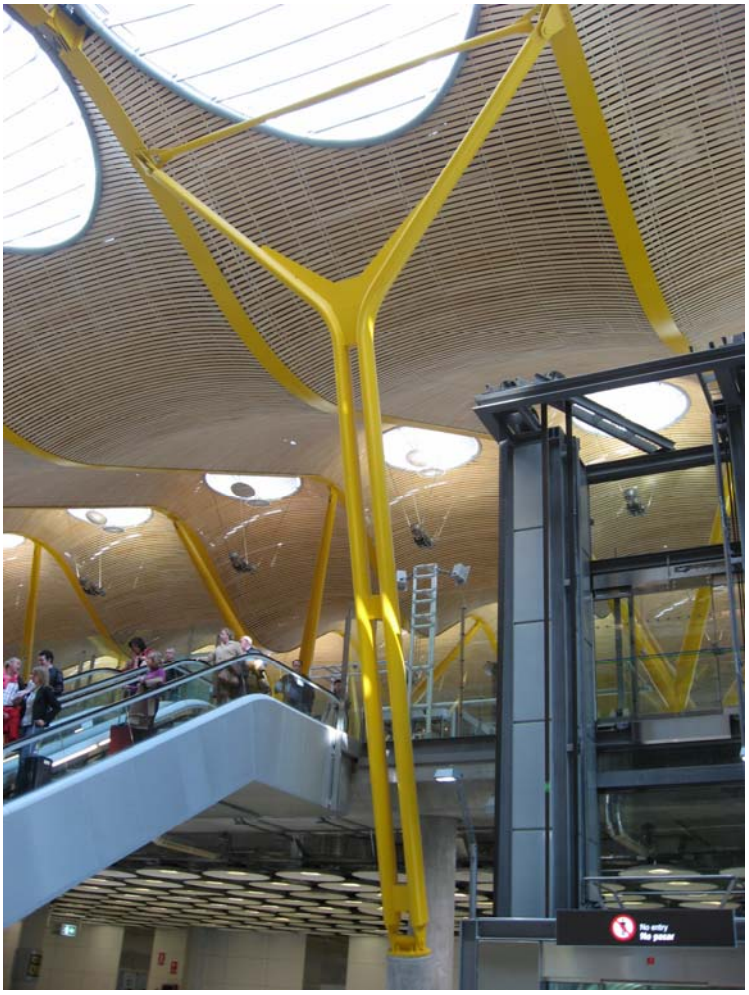

Fig. 3. Barajas Airport, Madrid (2004)

Fig. 4. Cork Airport, Ireland (2006)

Fig. 5. Heathrow Airport, London (2007)

Fig. 6. Heathrow Airport (detail), London (2007)

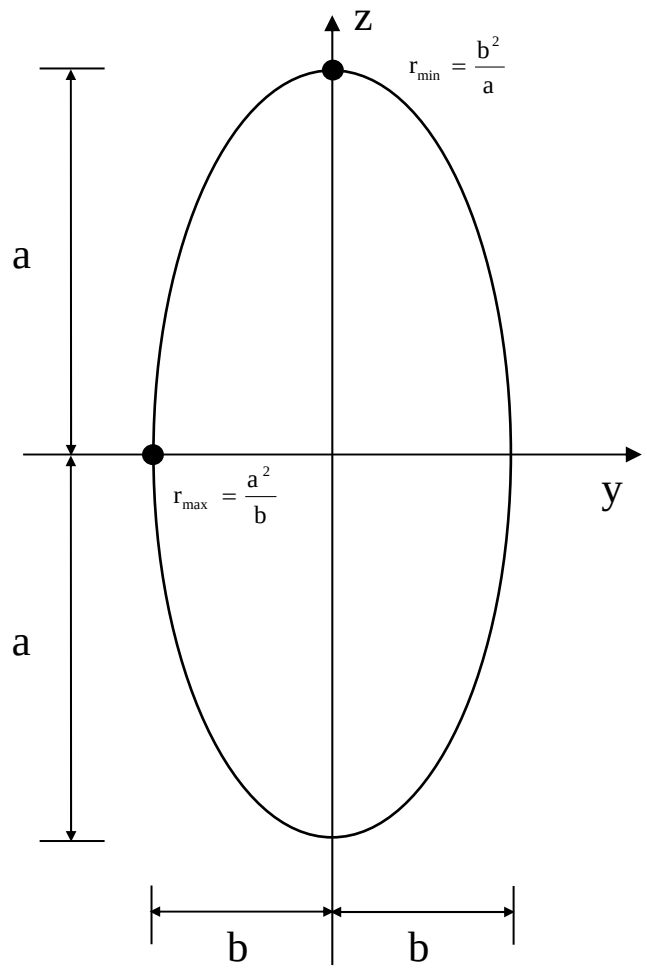

Fig. 7. Geometry of an ellipse

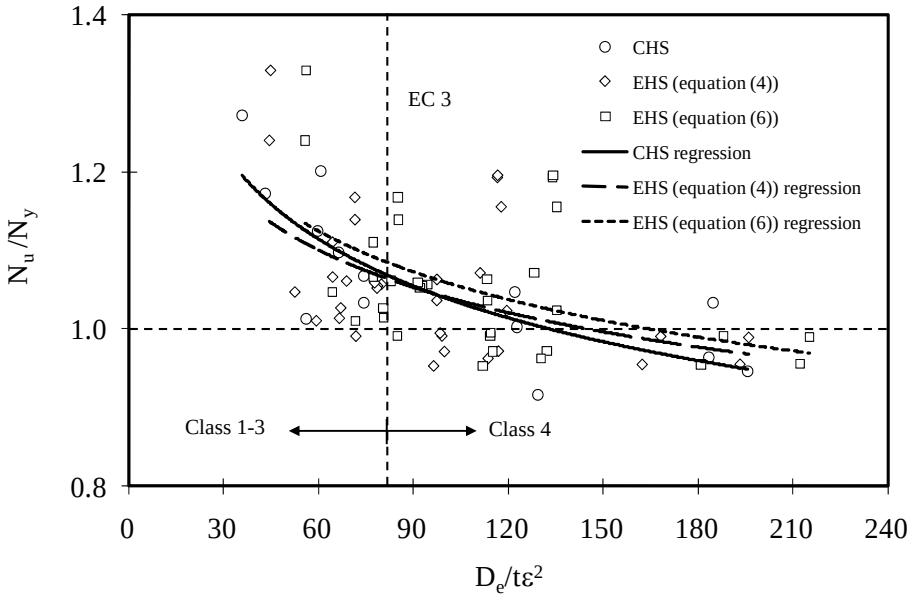

Fig. 8. Comparison of different equivalent diameters employed in EHS slenderness parameters

Fig 9. Typical cross-section failure mode in compression

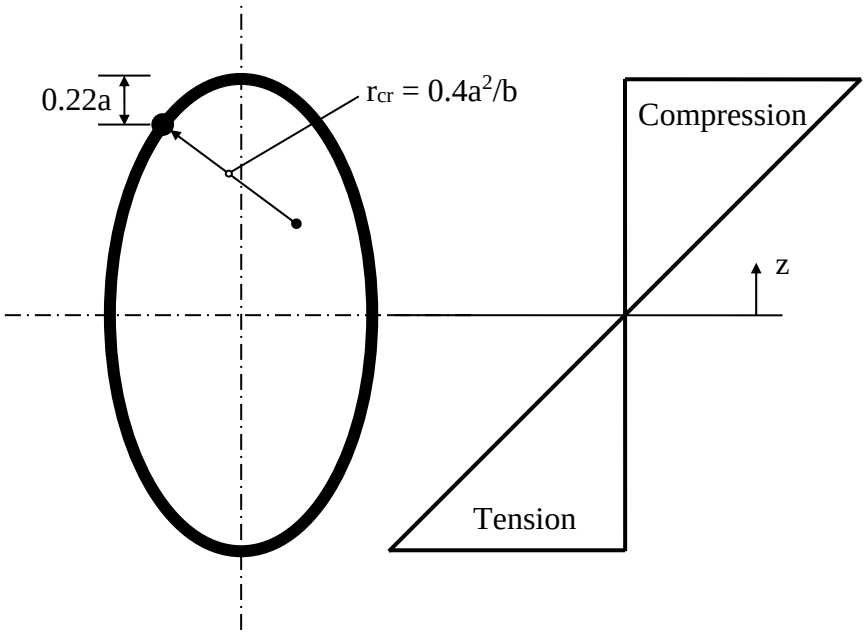

Fig. 10. Modified location of critical radius of curvature for EHS with a/b = 2 in major axis bending

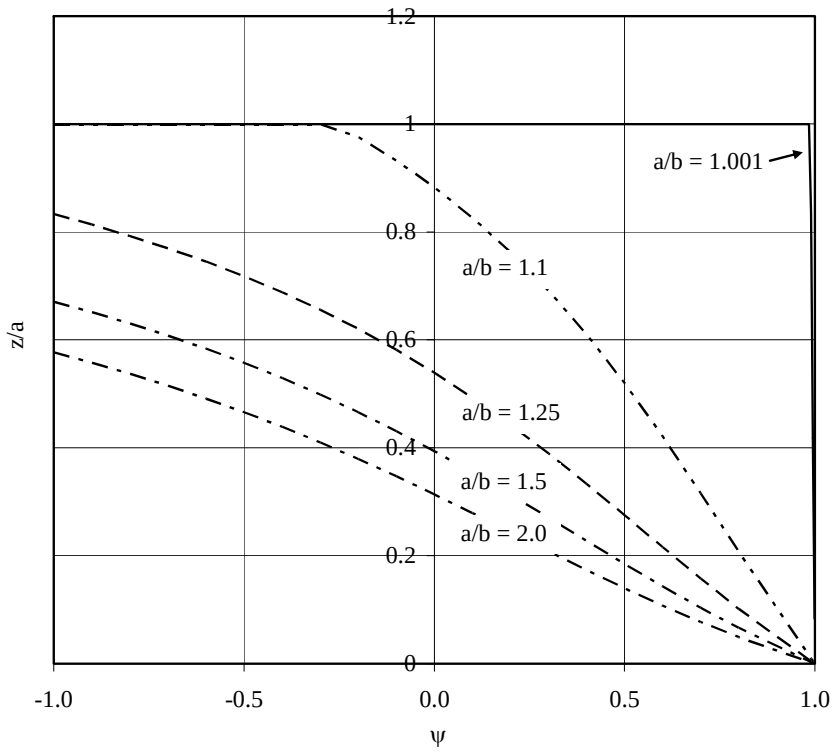

Fig. 11. Theoretical variation in position of r_{cr} with aspect ratio a/b and stress distribution ψ

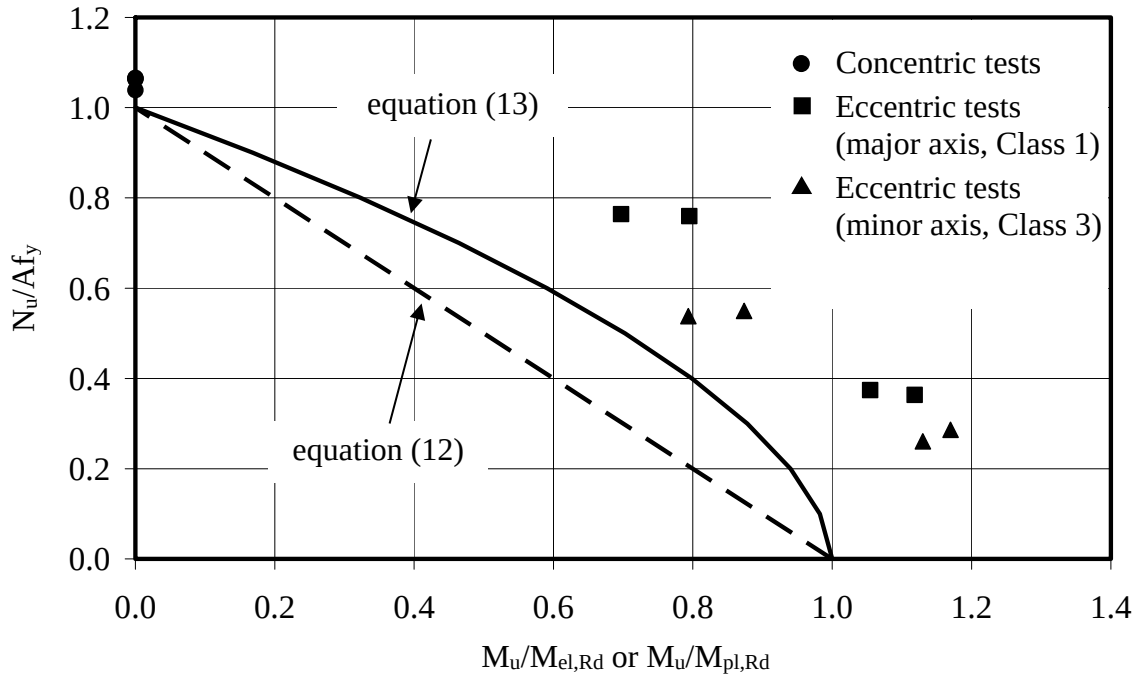

Fig. 12. Test results and interaction curves for combined bending and axial compression

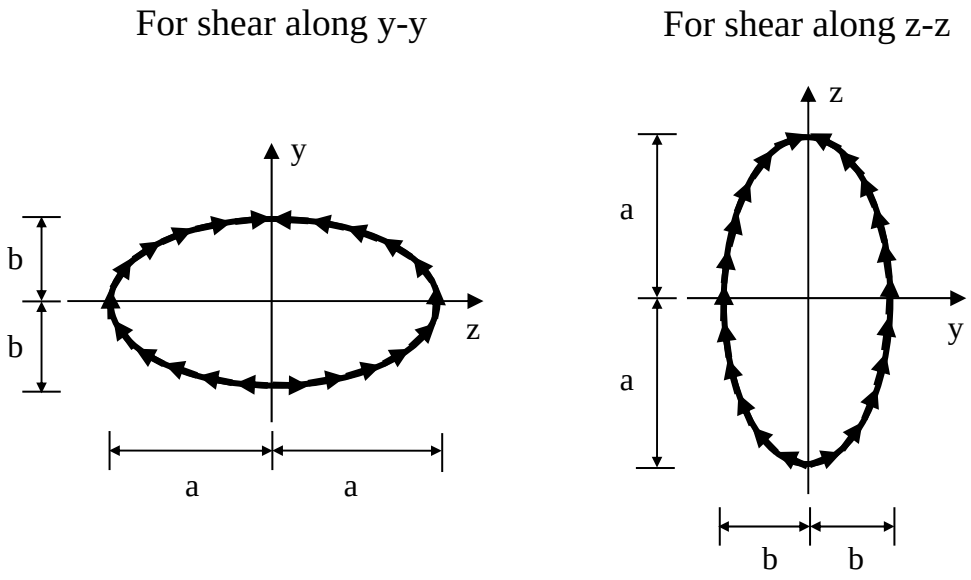

Fig. 13. Derivation of plastic shear area for EHS

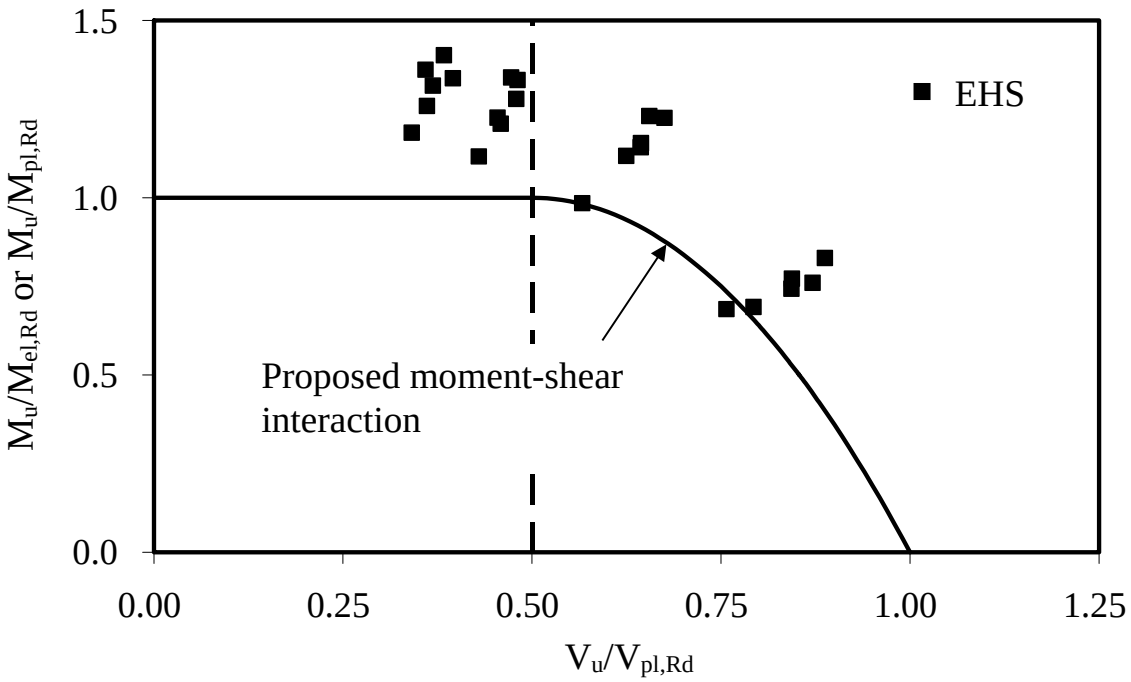

Fig. 14. Test results and interaction diagram for EHS under combined bending and shear

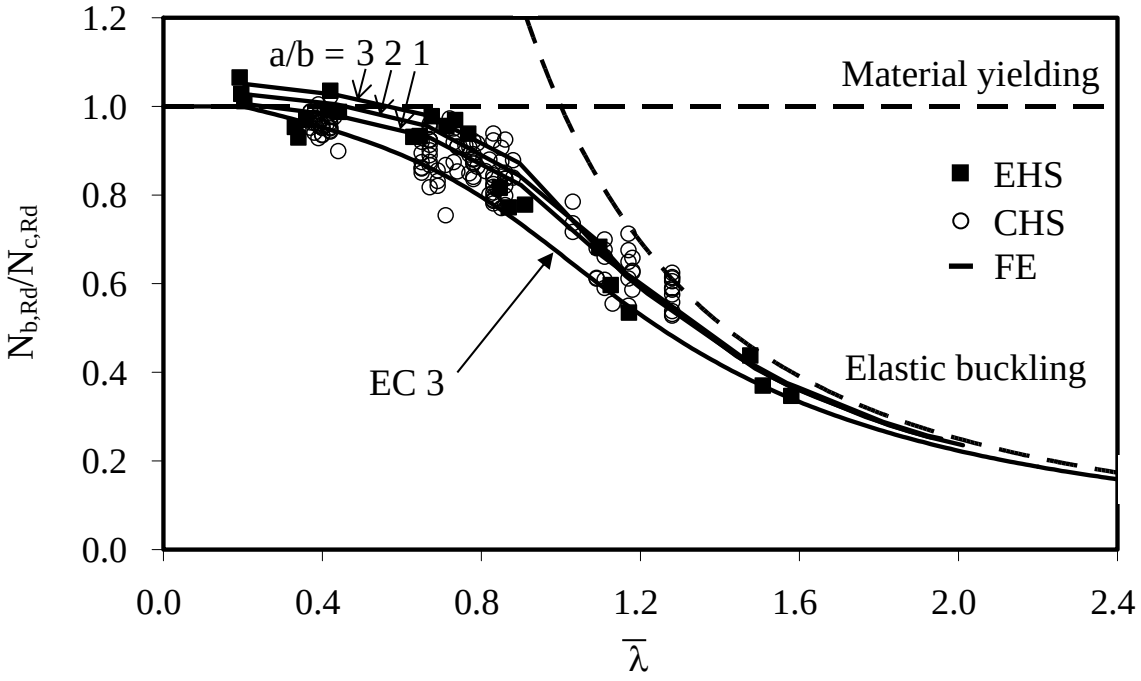

Fig. 15. EHS column buckling test results and proposed design curve

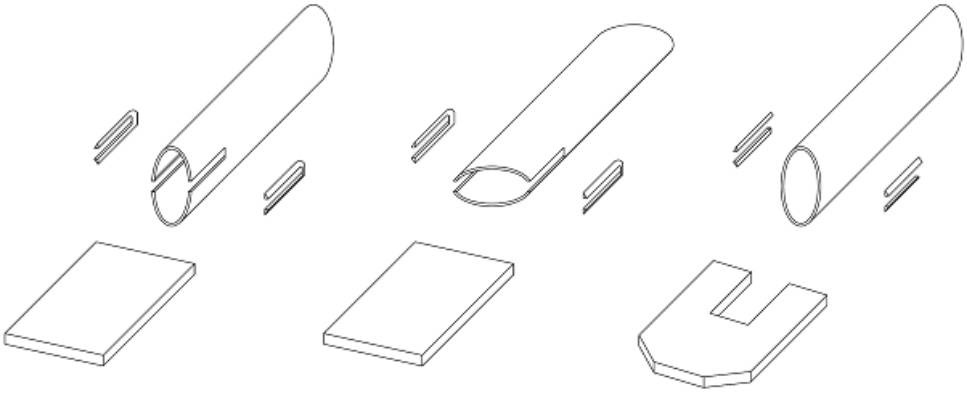

Fig. 16. Slotted end EHS connections

Table 1. Summary of experiments performed on elliptical hollow sections

Structural configuration			Structural carbon steel		Stainless steel	
			No. of tests	References	No. of tests	References
Cross-section tests	Compression	Unfilled	33	[23, 24]	6	[20]
		Concrete filled	42	[24, 47]	6	[22]
	Bending and combined bending + shear	Minor axis	23	[32, 36]	3	[21]
		Major axis	19	[32, 36]	3	[21]
Member buckling tests	Compression	Minor axis	12	[37]	4	[20]
		Major axis	12	[37]	2	[20]
Connection tests	Fully welded truss-type connections		7	[38, 39]		
	Gusset plate connections	Branch and through plate connections	6	[42]		
		End connections	5	[43]		
Total number of tests performed			159		24	